Resolution of Electrogenic Steps Coupled to Conversion of Cytochrome *c* Oxidase from the Peroxy to the Ferryl−Oxo State†

Sergey Siletsky, Andrey D. Kaulen, and Alexander A. Konstantinov*

A. N. Belozersky Institute of Physico-Chemical Biology, Moscow State University, Moscow 119899, Russia

Received November 3, 1998; Revised Manuscript Received February 2, 1999

ABSTRACT: Charge translocation across the membrane coupled to transfer of the third electron in the reaction cycle of bovine cytochrome *c* oxidase (COX) has been studied. Flash-induced reduction of the peroxy intermediate (P) to the ferryl−oxo state (F) by tris-bipyridyl complex of Ru(II) in liposome-reconstituted COX is coupled to several phases of membrane potential generation that have been time-resolved with the use of an electrometric technique applied earlier in the studies of the ferryl−oxo-to-oxidized (F → O) transition of the enzyme [Zaslavsky, D., et al. (1993) *FEBS Lett. 336*, 389−393]. As in the case of the F → O transition, the electric response associated with photoreduction of P to F includes a rapid KCN-insensitive electrogenic phase with a τ of 40−50 μs (reduction of heme *a* by Cu_A) and a multiphasic slower part; this part is cyanide-sensitive and is assigned to vectorial transfer of protons coupled to reduction of oxygen intermediate in the binuclear center. The net KCN-sensitive phase of the response is ∼4-fold more electrogenic than the rapid phase, which is similar to the characteristics of the F → O electrogenic transition and is consistent with net transmembrane translocation of two protons per electron, including vectorial movement of both "chemical" and "pumped" protons. The protonic part of the P → F electric response is faster than in the F → O transition and can be deconvoluted into three exponential phases with τ values varying for different samples in the range of 0.25−0.33, 1−1.5, and 6−7.5 ms at pH 8. Of these three phases, the 1−1.5 ms component is the major one contributing 50−60%. The P → F conversion induced by single electron photoreduction of the peroxy state as studied in this work is several times slower than the P → F transition resolved during oxidation of the fully reduced oxidase by molecular oxygen. The role of the Cu_B redox state in controlling the rate of P → F conversion of heme a_3 is discussed.

Cytochrome *c* oxidase (COX)[1] is a terminal enzyme of the mitochondrial respiratory chain (reviewed in refs *1*−*4*). It accepts electrons from ferrous cytochrome *c* and transfers them to molecular oxygen. The highly exergonic four-electron reduction of O_2 to two molecules of H_2O is coupled to transfer of protons across the membrane.

$$4c^{2+} + O_2 + 8H^+_{in} = 4c^{3+} + 2H_2O + 4H^+_{out}$$

During the full turnover of COX, four protons are transferred electrogenically from the mitochondrial matrix to the protein-buried oxygen-reducing center and are consumed in the water that is formed (so-called "chemical" or "substrate" protons), and four more protons are translocated all the way through across the membrane ("pumped" protons). The molecular mechanism of the redox-linked electrogenic transfer of the chemical and pumped protons has been a basic problem in the studies of the cytochrome oxidase mechanism for more than 20 years.

The sequence of intermediates in the COX-catalyzed reaction can be described by a simplified scheme

$$\begin{aligned} &\text{O (oxidized; } Fe^{3+}) \xrightarrow{\text{first two e}^-} \text{R (reduced; } Fe^{2+}) \xrightarrow{O_2} \\ &\qquad \text{Oxy (oxygenated; } Fe^{2+}{-}O_2) \rightarrow \text{P (peroxy;} \\ &\qquad Fe^{3+}{-}O_2{}^{2-} \text{ or } R^+Fe^{4+}{=}O^{2-}) \xrightarrow{\text{third e}^-} \\ &\text{F (ferryl−oxy; } Fe^{4+}{=}O^{2-}) \xrightarrow{\text{fourth e}^-} \text{O (oxidized; } Fe^{3+}) \end{aligned} \quad \text{(I)}$$

in which the redox or ligand state of heme a_3 iron is considered.

Following transfer of the first two electrons and addition of oxygen in the so-called eu-oxidase phase of the reaction cycle (*5*, *6*), COX forms two relatively stable oxygen intermediates usually termed "peroxy" (P) and "ferryl−oxo" (F) states. In a difference absorption spectrum versus the oxidized state, intermediate P is characterized by an α-maximum at 607 nm ($\Delta\epsilon$ = 10−12 mM^{-1} cm^{-1}) and a much weaker β-band at about 565 nm (*7*−*9*). As indicated in scheme I, P can be either an iron−peroxy complex or a ferryl−oxo intermediate (see refs *10* and *11*, and ref *12* for opposing views) analogous to compounds 0 and I of peroxidases, respectively (*5*, *6*); in either case, P is two-electron-deficient relative to the ferric (O) state. Intermediate F, which is one-electron-deficient relative to the O state,

† Supported by the Grants from the Russian Fund for Basic Research (97-04-49765 and 97-04-49144) and NIH Fogarty International Research Collaboration Award TW 00349.

* To whom correspondence should be addressed. Fax: +(7-095)-939-03-38. Telephone: +(7-095)-939-53-60. E-mail: konst@libro.genebee.msu.su.

[1] Abbreviations: COX, cytochrome *c* oxidase; RuBpy, tris-bipyridyl complex of Ru(II); O, P, and F, oxidized, peroxy, and ferryl−oxo forms of cytochrome oxidase, respectively.

10.1021/bi982614a CCC: $18.00
Published on Web 03/24/1999

displays an absorption maximum around 580 nm ($\Delta\epsilon \sim 5$ mM^{-1} cm^{-1}) and a β-band at about 535 nm. In the Soret region, both compounds show rather similar spectral characteristics, the heme a_3 band shifted from ca. 414 to 428 nm (*8*, *9*, *13*).

Originally, all four electrons transferred from cytochrome *c* to oxygen in the catalytic cycle of COX were considered to be equivalent with regard to their role in energy conservation by the enzyme (*14*). However, in 1989 Wikström reported (*15*) that each of the single-electron transitions P → F and F → O is coupled thermodynamically to translocation of 1.5−2 protons across the membrane of mitochondria, and since then proton pumping by COX has often been considered to be associated essentially or exclusively with single-electron redox transitions P → F and F → O in the binuclear oxygen-reactive center of the enzyme (*3*, *16*−*18*), i.e., to the transfer to oxygen of the third and fourth electrons [peroxidase phase of the cytochrome oxidase catalytic cycle (*5*, *6*)]. Recent studies with liposome-reconstituted COX indicate that the P → F → O part of the COX reaction cycle may be indeed associated with outward pumping of two H^+ per electron under steady-state conditions as compared to one H^+ per electron observed for the overall cytochrome oxidase reaction (*19*). Evidence for a major contribution of the P → F → O transitions to transmembrane charge translocation by COX has been obtained also on a single-turnover time scale (*20*, *21*). A number of hypothetical molecular mechanisms for the P → F and F → O proton pumping steps have been considered (*16*, *17*, *22*, *23*).

The P → F and F → O transitions are not elementary processes. According to current thinking, each of them involves several steps of vectorial intraprotein electron and proton transfer (*16*, *17*, *22*). It is obviously important to resolve these steps for understanding the proton pumping mechanism of cytochrome oxidase. Studies of this kind require a suitable method for rapid injection of a single electron into COX trapped at different intermediate states of the catalytic cycle before reduction.

In 1992, Nilsson (*24*) showed that a tris-bipyridyl complex of Ru(II) (RuBpy) binds electrostatically with COX at the cytochrome *c* docking site of the enzyme and, upon laser flash excitation, rapidly injects an electron into Cu_A. Starting with COX converted to the P or F state prior to photoexcitation, he was able to monitor individual P-to-F and F-to-O transitions on a time-resolved basis with the aid of optical absorption spectroscopy. In both compounds P and F, the photoreduced Cu_A transferred the electron to heme *a* in about 40−50 μs which was followed by reoxidation of heme *a* by the binuclear center. This reoxidation was reported to be biphasic with τ values of 0.3−0.8 and 3−5 ms.

Having combined this photochemical approach with a time-resolved electrometric technique developed by Drachev and collaborates (*25*−*27*), we were able to resolve earlier for the first time several intraprotein charge translocation steps coupled to the F → O transition (transfer of the fourth electron) in liposome-reconstituted bovine COX (*20*, *28*). Electrogenic reduction of heme *a* by Cu_A with a τ of 45 μs was demonstrated to be followed by two phases of electrogenic proton transfer provisionally assigned to uptake of a "substrate" proton with a τ of ∼1 ms and transmembrane proton pumping with a τ of ∼5 ms at pH 8. In recent collaborative research with the laboratory of Gennis, a similar triphasic pattern of charge translocation has been observed for the F → O transition of COX from *Rhodobacter sphaeroides* (*5*).

Here we describe the resolution of electrogenic steps associated with the transfer of the third electron, i.e., coupled to the P → F transition of COX. The results have been presented in a preliminary form at the 2nd European Biophysical Congress (*29*).

MATERIALS AND METHODS

RuBpy [tris(2,2′-bipyridyl)ruthenium(II) chloride hexahydrate] and decane (≥99% grade) were purchased from Aldrich, and collodion (Nitrocel-S) was purchased from Serva. Aniline (free base), stearylamine, and asolectin (phosphatidylcholine type II-S) were from Sigma. Egg yolk lecithin (grade 2a, chromatographically purified) was from Lipid Products (South Nutfield, Surrey, U.K.). H_2O_2 (30%, "Suprapur" grade) was from Merck. Other chemicals and biochemicals were from conventional sources such as Sigma, Merck, and Serva, as described previously (*20*, *28*).

COX isolated from beef heart mitochondria (*30*) and purified (*31*) was a kind gift from A. Kirichenko and T. Vygodina of this laboratory. The enzyme was reconstituted in phospholipid vesicles made from asolectin at a protein:lipid ratio of 1:40 with a cholate dialysis method (*32*). The enzyme (80−90%) is oriented in the vesicles as in mitochondria with the cytochrome *c* binding side facing outward, as checked by the reducibility of heme *a* by ascorbate and ruthenium hexammine or cytochrome *c* in the presence of KCN (e.g., see Figure 1 in ref *33*). It is noteworthy that since RuBpy dication is membrane-impermeable, only the mitochondrially oriented COX is reduced photochemically in our experiments.

The concentration of COX was determined from the absorption difference spectra (dithionite-reduced minus ferricyanide-oxidized) using a molar extinction value $\Delta\epsilon_{605-630}$ of 27 mM^{-1} cm^{-1} or in the presence of cyanide ($\Delta\epsilon_{605-630}$ = 21 mM^{-1} cm^{-1}).

Static absorption measurements of COX reconstituted in liposomes were carried out in an SLM-Aminco DW2000 UV/VIS dual-wavelength/split beam spectrophotometer.

Photoreduction of COX by RuBpy was induced by 15 ns (half-width) light pulses from a Nd:YAG laser Quantel 481 (Santa Clara, CA) operated at a doubled-frequency mode (λ = 532 nm; ∼50 mJ per flash).

Electrometric Measurements. The method and device for electrometric measurements of $\Delta\psi$ generation by energy-transducing proteins were developed originally by Drachev and collaborates for bacteriorhodopsin and bacterial reaction center experiments (*25*−*27*) and were adapted later for COX studies (*5*, *20*). Experiments were carried out in home-built Teflon electrometric cells. The cell was comprised of two 4.5 mL compartments, each with a quartz optical window. A small opening in a partition between the two compartments of the cell was sealed by a collodion film, presoaked in a decane solution of egg yolk lecithin (100 mg/mL) and stearylamine (1 mg/mL). Cytochrome oxidase vesicles adhered to one side of the collodion film. To this end, the two compartments of the cell were filled in with a buffer containing 30 mM $MgSO_4$ and 10 mM HEPES buffer (pH 7.5). Cytochrome oxidase vesicles were added to the sample

compartment (final concentration of ~1 mg of protein/mL) and adhered spontaneously to the collodion film during the course of an ~3 h incubation at room temperature. After completion of the procedure, the cell was carefully refilled with the final reaction buffer [typically, 5 mM Tris-acetate (pH 8) with 10 mM aniline]. This was carried out simultaneously for the sample and reference compartments with the aid of a dual-channel peristaltic pump. During this procedure, the unattached cytochrome oxidase vesicles were removed from the sample compartment and only the collodion film-adhered proteoliposomes remained. All subsequent additions (e.g., RuBpy) were made symmetrically to both compartments. Since the complex of RuBpy with COX is essentially electrostatic, the low ionic strength of the solutions is a prerequisite in the photoreduction experiments, and following the methods described in ref *24*, 5 mM Tris-acetate (pH 8) has been used as the basic buffer for the electrometric measurements, if not indicated otherwise.

Charge transfer across the membrane of the collodion film-adhered phospholipid vesicles results in an electric potential difference generated between the two film-insulated compartments (see the equivalent electric scheme in refs *26* and *34*), and this voltage was measured with a pair of light-protected Ag/AgCl electrodes. The electric signal was passed through an operational amplifier (Burr-Brown 3554) and fed into a PC-interfaced digital transient recorder Datalab-1080 (Dataloop). The effective time resolution of the setup was 50 ns/point as limited by the operational amplifier.

The excitation light from the laser was projected at the collodion film with the attached cytochrome oxidase vesicles through a quartz optical window in the cell. The effective "quantum yield" (yield per flash) of the RuBpy-mediated photoreduction of Cu_A with excitation at 532 nm is very low partly due to the low absorptivity of RuBpy at this wavelength. Only 2−3% of COX was photoreduced per flash as described in ref *24*, and the yield may be even smaller in our experiments due to a ca. 4-fold lower energy of the flash. The electric response decreases linearly with decreasing flash energy. Presumably, only a small fraction of the film-adhered cytochrome oxidase vesicles respond to each flash and the photoelectric trace amplitude was typically <5 mV, whereas flash-induced electric responses as high as 120−150 mV could be observed in this system with bacteriorhodopsin (*25*) or bacterial reaction center vesicles (*27*).

The electrometric cell was thermostated with an external water bath. With an improved sample holder used in this work, temperature and pH could be measured directly in the sample compartment.

COX was converted to the P state by aerobic bubbling of CO through the liposome-containing compartment of the electrometric cell for 1−2 min and to the F state by addition to this compartment of excess H_2O_2.

Deconvolution of the kinetic traces into individual exponentials was performed with the program Discrete (*35*). The program determines the minimal number of exponents sufficient for simulation of the experimental curve.

RESULTS

Hydrogen peroxide added to the oxidized COX converts the enzyme to a mixture of P and F states, the relative proportions of P and F depending on the peroxide concentration, pH, and some other conditions (*13*, *36*−*38*). In liposome-reconstituted COX at pH ≥8, low concentrations of peroxide (<200 μM) give rise to a steady state in which the contribution of P is typically around 40% while an increase in the peroxide concentration to several millimolar results in full conversion of COX to the F state (*13*, *36*, *39*).

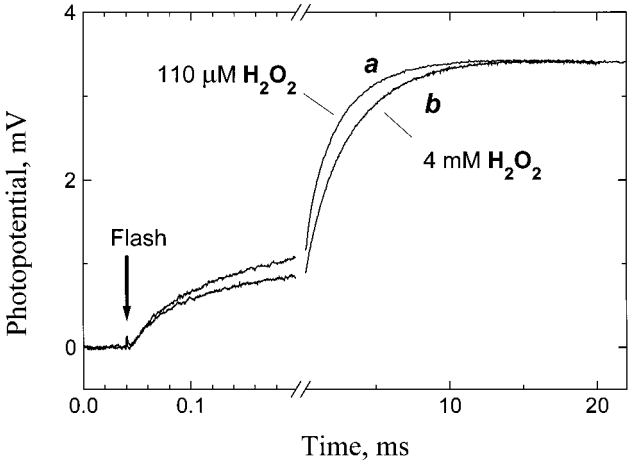

FIGURE 1: Kinetics of the flash-induced membrane potential generation by cytochrome *c* oxidase at low and high hydrogen peroxide concentrations. Conditions were 5 mM Tris-acetate buffer at pH 8.1; 40 μM RuBpy has been added as a photoreductant and 10 mM aniline as a sacrificial electron donor to make COX photoreduction irreversible. Prior to the flash, COX has been converted to a mixture of P and F states by addition of 0.11 mM hydrogen peroxide (trace a); after trace a was recorded, the hydrogen peroxide concentration was increased to 4 mM to obtain the pure F state of the enzyme (trace b).

It was noticed originally in this group that charge translocation by COX induced by single-electron photoreduction of the enzyme preincubated with hydrogen peroxide decelerates with increasing H_2O_2 concentrations (*40*). Results of a typical experiment of this kind made in collaboration with Zaslavsky are shown in Figure 1. It can be seen that at 110 μM H_2O_2, the photoelectric trace is markedly faster than in the presence of 4 mM peroxide. The difference is confined to the KCN-sensitive (protonic) phase of the reaction, indicating that proton translocation in the P → F conversion may be faster than for the F → O conversion. However, even at low H_2O_2 concentrations, the contribution of compound F is quite significant which renders quantitative interpretation of the data difficult.

To minimize the contribution of the F state, we have used another method of compound P generation based on bubbling of CO through the aerobic solution of ferric COX (*41*). Presumably, CO serves as a two-electron donor for the binuclear center, and subsequent interaction of the doubly reduced a_3-Cu_B center with atmospheric O_2 produces stable compound P. At weakly alkaline pH, the method gives a decent steady-state yield of the P state (60−90% of the total enzyme concentration as reported by different authors) and, importantly, does not generate F to any significant extent (*8*, *9*). Therefore, after aerobic bubbling of CO, a mixture of P and O states of COX is obtained, as opposed to a combination of P and F states generated by hydrogen peroxide addition. Admixture of the O state raises much fewer problems than contamination with F because single-electron reduction of the O form is not associated with the KCN-sensitive electrogenic proton transfer steps but only

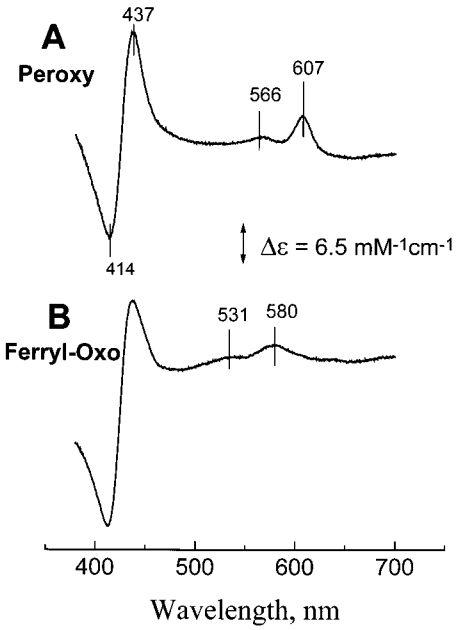

FIGURE 2: Generation of compounds P and F of liposome-reconstituted COX. (A) Compound P. Cytochrome oxidase proteoliposomes (1.2 μM in COX) were incubated for 20 min in the buffer [75 mM $K_2H_2PO_4$ and 1 mM $MgSO_4$ (pH 8.0)] supplemented with 100 μM ferricyanide and 10 nM catalase, and the absorption spectrum of the suspension was taken as a baseline. CO was bubbled through the aerobic suspension for 1 min, and the absorption difference was recorded in ~3 min. The presence of catalase had no any noticeable effect on the CO-induced spectrum. (B) Compound F. The conditions were like those described for panel A, the differences being that 4 mM H_2O_2 was added to the sample instead of the CO bubbling and there is no catalase in the reaction mixture.

with the cyanide-insensitive microsecond phase of heme *a* reduction by Cu_A (*20*). The contribution of the O state fraction to the overall photoelectric trace is therefore easy to extract, and in contrast to that of compound F, it does not interfere with the electrogenic proton transfer steps coupled to single-electron reduction of P.

Figure 2A shows absorption changes induced by aerobic treatment of liposome-reconstituted COX with carbon monoxide. In the visible region, the difference spectrum shows an α-peak at 607 nm with a β-band at 566 nm and an α:β amplitude ratio of ~1:4 that is typical of compound P (*9*, *38*). The molar extinction at 607 nm (ca. 6 mM^{-1} cm^{-1}) indicates conversion of about 60% of the enzyme to the P state. Accordingly, the Soret response shows a peak-to-trough amplitude of 30 mM^{-1} cm^{-1} consistent with 60% conversion of heme a_3 to the P state if compared to the $\Delta\epsilon$ value of ~50 mM^{-1} cm^{-1} (*9*, *42*). The line shape of the difference spectrum shows that there is no significant contribution of the F state under these conditions. In agreement with the earlier experiments with liposome-reconstituted COX (*13*, *36*), addition of 4 mM hydrogen peroxide to cytochrome oxidase vesicles results in conversion of the enzyme to the F state as evidenced by the peak at 580 nm with a β-band at 531 nm (Figure 2B). The difference spectra given in panels A and B of Figure 2 were obtained with different samples because the catalase present in the experiments whose results are shown in Figure 2A precludes probing the effect of H_2O_2 addition. The same pair of difference spectra can be observed in one sample if the aerobic CO treatment is carried out in the absence of catalase.

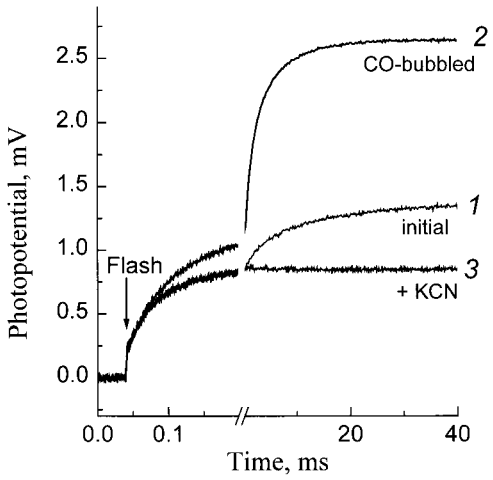

FIGURE 3: Membrane potential generation coupled to single-electron photoreduction of liposome-reconstituted COX. Tris-acetate buffer (5 mM, pH 8.1) with 40 μM RuBpy and 10 mM aniline. t = 19 °C. The traces were recorded consecutively with the same sample in the following order: (1) after incubation for 20 min with 200 μM ferricyanide and 10 nM catalase, (2) 5 min after bubbling with CO for about 1 min, and (3) after addition of 0.5 mM KCN.

Figure 3 shows kinetics of charge translocation across the proteoliposome membrane induced by single-electron photoreduction of COX by RuBpy. In the vesicles treated with ferricyanide and catalase to provide for the oxidized state of the enzyme and remove trace amounts of H_2O_2 potentially present in the reaction mixture (trace 1), photoreduction results in an increase in the membrane potential (negative inside proteoliposomes) dominated by a 45 μs phase that is insensitive to KCN and can be attributed to oxidation of Cu_A by heme *a* (*20*). In addition, there is a minor millisecond part of the response; this part, also observed previously (*20*), is fully suppressed by KCN (not shown) and presumably originates mainly from proton translocation in a small fraction of COX present initially in the P or F state. Contamination of the "as-isolated" enzyme by P and F forms has been noticed by several groups (*38*, *43*) and is even more probable in the case of membrane-reconstituted COX where the phospholipid environment can provide a source of slow electron leak through the enzyme. The presence of the P state in the aerobically oxidized liposome-reconstituted COX is evident for instance from the data given in Figure 1A of ref *13*, where a trough at 607 nm in the difference absorption spectrum had been observed upon addition of excess H_2O_2 to the oxidized liposome-bound enzyme.

In both the F → O and P → F steps, the amplitude of the slow KCN-sensitive part of the photoelectric response is about 4-fold larger than that of the rapid phase (cf. ref *20* and below). Since the partial contribution of the KCN-sensitive phase in trace 1 of Figure 3 is about $^1/_2$ of that of the rapid phase, the fraction of the endogenous (F and P) states can be evaluated as $^1/_2 \times {}^1/_4$ (≈12%). Curve fitting shows however that about $^1/_3$ of the KCN-sensitive phase in trace 1 is due to very slow secondary processes (trace 1 in Figure 3 does not reach a plateau even at 40 ms) that are not observed during photoreduction of either F or P states of the enzyme (e.g., Figure 5A). Therefore, the actual contribution of P and F may be around 8%, in excellent agreement with the observations of other workers (*38*).

Table 1: Comparison of Electrogenic Responses in the P → F and F → O Transitions of COX[a]

electrogenic phase	F to O[b]	P to F[c]
KCN-sensitive	rapid	
	$\tau_1 = 44\ \mu$s (36−48)	$\tau_1 = 47\ \mu$s (44−50)
	$\alpha_1 = 0.21$ (0.19−0.25)	$\alpha_1 = 0.32$ (0.29−0.35)[d]
		α_1(corrected) = 0.21
KCN-insensitive		
	intermediate	$\tau_2 = 0.3$ ms (0.25−033)
	$\tau_2 = 1.1$ ms (0.9−1.3)	$\alpha_2 = 0.16$ (0.12−0.21)[d]
	$\alpha_2 = 0.22$ (0.19−0.25)	α_2(corrected) = 0.18
		$\tau_3 = 1.3$ ms (1−1.5)
		$\alpha_3 = 0.38$ (0.34−0.41)[d]
	slow	α_3(corrected) = 0.43
	$\tau_3 = 5.1$ ms (4.3−5.6)	
	$\alpha_3 = 0.57$ (0.5−0.6)	$\tau_4 = 6.8$ ms (6−7.5)
		$\alpha_4 = 0.16$ (0.11−0.23)[d]
		α_4(corrected) = 0.18

[a] Experimental traces used for curve fitting in the case of the P → F transition correspond to trace 2 in Figure 3 as reproduced with three different preparations of proteoliposomes. The α (fractional amplitude) and τ ($t_{1/e}$) values are given as average values with the maximal deviation interval in parentheses. The scatter for repetitive measurements with the same sample is negligible. [b] Data from ref *20*. [c] Data from this work. [d] The observed α values are distorted due to incomplete conversion of COX to the P state during the CO bubbling procedure, i.e., by contribution from single-electron reduction of state O (see the text). The mean values corrected for 60% yield of the P state are given as α(corrected) values and are discussed in the text. The τ values do not require correction.

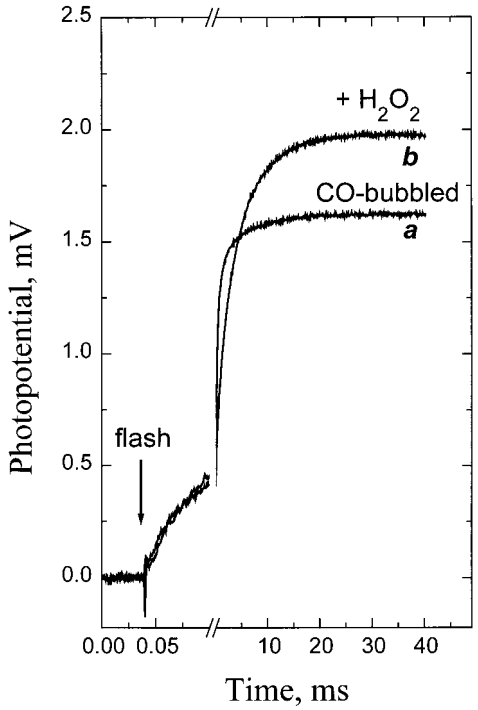

FIGURE 4: Comparison of electrogenic responses of COX bubbled with CO (a) and treated with H_2O_2 (b). Conditions were 5 mM Tris-acetate buffer (pH 8.1) with 40 μM RuBpy and 10 mM aniline; $t = 20$ °C. Trace a was recorded in 3 min after bubbling the open sample compartment of the electrometric cell with CO. After trace a was recorded, 4 mM H_2O_2 was added to both compartments and trace b recorded in about 3 min. The traces are given as registered without normalization, and curve fitting resolves the same absolute amplitude of the rapid phase (0.46 ± 0.01 mV). The relative contribution of the rapid phase is 30% in trace a and 22% in trace b.

The millisecond part of the photoelectric response greatly increases upon aerobic bubbling of CO through the suspension of cytochrome oxidase vesicles (Figure 3, trace 2). This millisecond phase is fully abolished by KCN (Figure 3, trace 3) which reacts rapidly with the P state of COX (*8*), converting the enzyme to the ferric cyanide complex. Single-electron photoreduction of the latter by RuBpy is associated with the 45 μs electrogenic phase only (*20*) and, on a millisecond time scale, is confined to reduction of heme *a*, although much slower electron leak to Cu_B (minutes; *44*) cannot be excluded.

The relative amplitude of the 45 μs electrogenic phase in the photoelectric responses of CO-bubbled cytochrome oxidase was around 30% (see Table 1), notably higher than the value of ∼20% that is typical of the F → O transition as measured earlier (*20*) or in this work (data not shown). However, spectrophotometric controls show reproducibly that in the CO-bubbled cytochrome oxidase vesicles, only 55−60% of COX is converted to the P state with the rest of the enzyme remaining in the oxidized form (e.g., Figure 2A). Therefore, the rapid KCN-insensitive phase of membrane potential generation by CO-bubbled vesicles contains a 40−45% contribution from COX in the O state. Subtraction of this contribution from the overall trace reduces the relative amplitude of the 45 μs phase in the P → F transition from the average value of 32 to 21% (see Table 1). In other words, the amplitude of the cyanide-sensitive protonic phase in the P → F transition is about 4-fold higher than the amplitude of the 45 μs electrogenic phase. The same amplitude ratio of 4:1 for the cyanide-sensitive and cyanide-insensitive electrogenic phases was observed earlier for the F → O transition (*20*). The similar electrogenicity of the P → F and F → O transitions is also evidenced by the observation that titration of the photoelectric response by increasing concentrations of H_2O_2 (i.e., transition from a roughly equimolar mixture of P and F states to pure F) results in deceleration of the KCN-sensitive part of the traces but does not affect the amplitude of the response to any significant extent (Figure 1; *40*).

In Figures 4 and 5, electrogenic responses of COX bubbled with CO are directly compared with the photoelectric traces observed in the F → O transition of the enzyme. The data obtained in several experiments with different samples are summarized in Table 1.

In the experiment whose results are shown in Figure 4, the two photoelectric responses have been recorded with the same sample, first bubbled aerobically with CO and then treated with excess H_2O_2 to convert COX to the F state. The traces are given without any normalization. It can be seen that addition of H_2O_2 to the CO-bubbled sample does not affect an amplitude of the rapid phase (0.46 ± 0.01 mV as resolved by curve fitting) but increases the slow KCN-sensitive part of the response. If the CO-bubbled sample were 100% in the peroxy state, such a result could mean that the cyanide-sensitive phase in the F → O transition is more electrogenic than in the P → F step. However, as discussed above, part of COX after aerobic bubbling with CO remains in the O state, single-electron reduction of which is coupled only to the 45 μs electrogenic phase. This "idle" fraction is converted by excess H_2O_2 to the ferryl−oxo state, leading to an increased overall electrogenicity of photoreduction. If we assume as above 60% occupancy of the P state in the

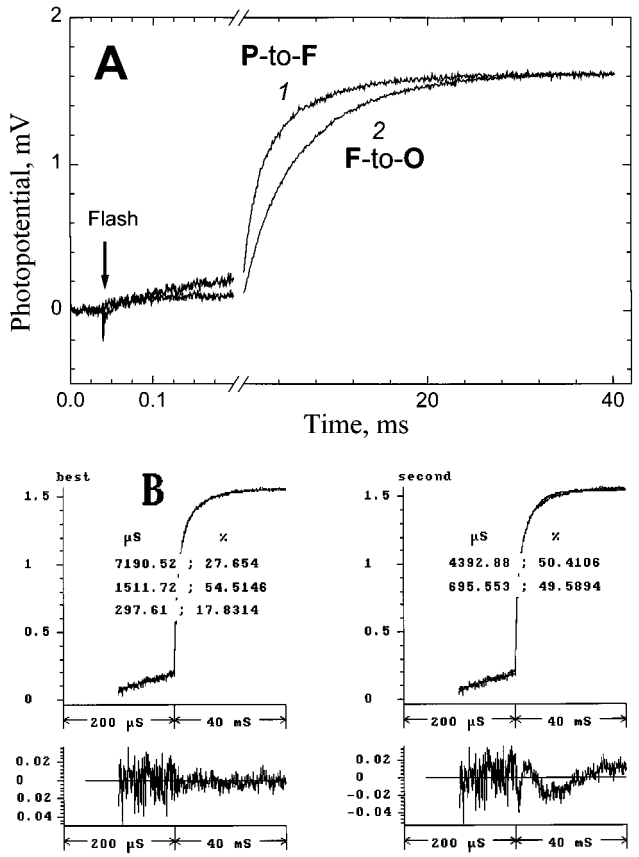

FIGURE 5: Kinetics of the KCN-sensitive electrogenic proton translocation by COX in the P → F transition. (A) Comparison of intraprotein proton transfer in the P → F and F → O transitions. (1) CO-bubbled cytochrome oxidase vesicles, with conditions as described for trace 2 in Figure 3. (2) COX converted to the F state by addition of 4 mM hydrogen peroxide. The KCN-insensitive 45 μs phase was subtracted from both traces, and the remaining KCN-sensitive parts were normalized (trace 2 was multiplied by a factor of 1.3) to facilitate visual comparison of the kinetics. (B) A typical curve fitting of the kinetics of the electrogenic proton transfer coupled to the P → F transition of COX. The figure reproduces a standard format of a curve fitting printout. The two upper panels show the same experimental trace (obtained as described for trace 2 in Figure 3, except that catalase was not added in this particular experiment) together with the theoretical curves drawn through it in accordance with the results of the deconvolution. The contribution of the 45 μs KCN-insensitive phase of the response was resolved and subtracted from the trace (as described for panel A) prior to the analysis of the KCN-sensitive part, as it improves stability of the curve fitting procedure significantly. In the left panel is shown the best fit (three exponents). In the right panel is shown the second to the best fit (two exponents). A single-exponent fit was very poor and has been omitted. Parameters of the resolved exponents are printed out in the upper panels (left column, τ values in microseconds; right column, fractional contributions in %). The lower panels give the plots of the residuals to better illustrate quality of the fitting.

CO-bubbled sample, the peroxide-induced increment of the slow phase will correspond to the cyanide-sensitive phase in the P → F transition being 4.1-fold more electrogenic than the rapid phase in this particular experiment.

In Figure 5, we compare the kinetics of the protonic parts of the electric responses of COX in the samples bubbled with CO (a mixture of P and O states, trace 1) and treated with H_2O_2 (virtually pure F state, trace 2). The rapid electrogenic phase with a τ varying in the 40−50 μs range does not depend noticeably on whether heme a_3 is in the free ferric, ferryl−oxo, peroxy, or CN^--bound state, and the contribution of this phase is resolved easily by addition of KCN or by initial preliminary curve fitting. Therefore, to refine the analysis, we subtracted this phase from the experimental traces (e.g., in Figure 5A**)** which improves considerably fitting of the remaining protonic cyanide-sensitive parts of the curves. Note that this procedure eliminates the contribution of the O-state fraction to the electrogenic response of the CO-bubbled sample. The KCN-sensitive parts of the photoelectric traces in the millisecond range have been normalized to facilitate visual comparison of the kinetics.

It can be seen that the KCN-sensitive protonic part of the photoelectric response coupled to single-electron reduction of the P state is significantly faster than that observed for the enzyme in the F state. This has been observed consistently in all experiments with different preparations of COX. A more detailed comparison based on curve deconvolution into individual exponents is described below.

Representative results of curve fitting of the photoelectric responses associated with the P → F transition are given in Figure 5B. First of all, the cyanide-sensitive phase cannot be fitted satisfactorily by a single exponent (the fitting not shown) and obviously includes several components. If by analogy with the F → O transition (*5*, *20*) analysis of the KCN-sensitive part of the curve is confined to two exponents (i.e., to three exponents for the overall curve including the microsecond phase), the fit is not that bad and the two phases show τ values of about 0.7 and 4.4 ms and equal amplitudes (Figure 5B, right panel; *29*). These τ values are similar to the time constants of the intermediate and slow electric phases resolved in the F → O transition [0.9−1.3 and 4.3−5.6 ms, respectively (*20*); see Table 1]. However, the intermediate:slow amplitude ratio in the case of the P → F transition is 1:1, while it is close to 1:3 for the F → O step (*20*); it is mainly this increased contribution of the intermediate phase that accounts for the faster overall photoelectric response of compound P as compared to that of compound F in Figure 5A.

The fit is markedly improved by approximation of the KCN-sensitive part of the photoelectric trace by three exponents (left panel). This has been observed for all the experimental P → F traces analyzed, whereas in the case of the F → O photoelectric traces, three-exponent fitting of the cyanide-sensitive part does not result in a superior fit. The three-exponent solution reveals a major phase with a τ of ∼1.5 ms (55% contribution), and two minor components with τ values of ca. 0.3 and 7 ms. The 1.5 and 7 ms components have no obvious counterparts in the curve fitting of heme *a* absorption changes in the experiments of Nilsson (*24*). The minor 0.3 ms electric component may be related to the 0.3 ms exponent resolved optically by Nilsson (*24*) and can also be compared to the electrogenic phase with a τ of ca. 0.2 ms assigned by the Helsinki group to the P → F transition during oxidation of the fully reduced enzyme by oxygen (*21*).

The signal-to-noise ratio of the photoelectric traces is remarkably good, and accordingly, for any particular trace, the parameters are fitted with high precision. However, the τ values of the three cyanide-sensitive electrogenic phases resolved by fitting of the photoelectric P → F curves obtained in experiments with different preparations of cytochrome oxidase vesicles varied in the range of 0.25−0.33, 1−1.5, and 6−7.5 ms (Table 1). We consider this scatter acceptable

for the purposes of this work. Notably, all three phases showed correlated behavior; i.e., for any particular curve, all three of them were slower or faster approximately to the same extent. At the same time, the time constant of the rapid phase remained in the range of 40−50 μs for all the samples (the scatter in this case reflects mainly the stability of the fitting procedure with no noticeable differences among the samples).

DISCUSSION

Comparison between the P → F and F → O Electrogenic Transitions. Our data show that conversion of cytochrome oxidase compound P to compound F induced by photoinjection of a single electron from RuBpy is coupled to intraprotein charge translocation directed across the membrane on a time scale consistent with enzyme turnover. To a first approximation, charge separation associated with the P → F transition is similar to that observed earlier for the F → O conversion (see Table 1). In both cases, the electric response is comprised of (i) a rapid phase with a τ of 40−50 μs that is insensitive to KCN and can be assigned to reduction of heme *a* by Cu_A (*5*, *20*, *24*, *28*) and (ii) a millisecond cyanide-sensitive proton translocation phase that is about 4-fold more electrogenic than the rapid phase and includes at least two components (*20*). The contribution of charged group movement inside the protein cannot be excluded. However, the three-dimensional structure of bovine COX in different redox and ligand-bound states (*45*) does not indicate any significant movements of this kind except for the redox-dependent change in the position of aspartate 51 at the P phase surface of subunit I.

Stoichiometry of Charge Translocation. Amplitudes of the electrogenic phases in our experiments give only relative values for the number of charges translocated at each of the steps. The Cu_A → heme *a* step (the 45 μs electrogenic phase) is well-resolved kinetically and can be used as an internal standard to calibrate other phases in the same photoelectric trace, as done earlier for the F → O transition of COX (*20*). As discussed in refs *20* and *23*, quantitation of the number of charges translocated in the cyanide-sensitive phases of the P → F or F → O transitions performed in this way depends critically on the electrogenicity assigned to the Cu_A → heme *a* reaction.

If we assume that electron transfer from Cu_A to heme *a* is essentially complete and is thermodynamically equivalent to translocation of one elementary charge across half of the dielectric barrier (*46*, *47*), the cyanide-sensitive vectorial proton transfer in the P → F transition will correspond to transmembrane translocation of two charges per electron (and the entire P → F step to transfer across the membrane of 2.5 charges), exactly as in the case of the F → O step (*20*). Note that this includes contributions from electrogenic transfer of both "chemical" and "pumped" protons.

There are two most obvious interpretations of such a stoichiometry. First, if one "chemical" proton is taken up electrogenically from the negative phase to the binuclear center in the P → F transition (*16*−*18*, *48*; but cf. ref *2*), our data may indicate additional transmembrane translocation of 1.5 protons at this step of the catalytic cycle rather than of two as implied by the "histidine cycle" model (*18*); this can be visualized for instance as transmembrane pumping of 1 proton plus release of 1 preloaded proton from the enzyme interior to the positive side (see ref *6* for a more detailed discussion). Second, it is possible that the P → F transition is coupled to transmembrane pumping of 2 protons in agreement with the histidine cycle (*18*), but in variance with this model (*18*), there is no *electrogenic* uptake of a "chemical" proton coupled to this reaction. Charge compensation at the oxygen intermediate site can be confined in this case to a local nonelectrogenic displacement of H^+ from some protonated group (proton trap) to the reduced oxygen intermediate.

The number of charges (protons) translocated in the P → F and F → O transitions as calculated from our data here and in ref *20*, respectively, can be lower if the Cu_A→ heme *a* redox step is coupled thermodynamically to transfer of less than 0.5 charge (see ref *23* for discussion) or/and if electron transfer from Cu_A to heme *a* in the 45 μs phase is not complete due to an insufficiently high E_m difference between these redox centers. Note that in the latter case, these are E_m values for Cu_A and heme *a* in the peroxy and ferryl−oxo states of COX that need to be considered. These values, in particular, the E_m of heme *a*, may be different from the conventional E_m values determined under the conditions where heme a_3 is in the ferric or ferrous state. An estimate of 53 mV for the E_m difference between heme *a* and Cu_A in the F state of COX has been reported very recently (*49*) and actually coincides with the ∼50 mV difference reported for the conventional oxidized state (see ref *50*); it corresponds to virtually complete (ca. 90%) oxidation of Cu_A by heme *a*. No corresponding data for the P state are yet available.

It must be emphasized that the influence of the above factors on the electrogenicity of the P → F and F → O transitions as calculated from our electrometric measurements is essentially the same with respect to both steps. Therefore, whatever the uncertainties in the absolute number of charges translocated, our data indicate that transfers of the third and fourth electrons in the COX catalytic cycle are very similar with respect to proton translocation efficiency. This is per se a useful result, allowing us to impose constrains on the choice among the many versions of the COX electrogenic mechanism. In particular, our data corroborate the model of Wikstrom (*15*), assigning similar electrogenicity to the P → F and F → O steps, and are more difficult to reconcile with the mechanism suggested recently by Michel (*23*) [see also the commentary to this paper (*51*)] which postulates that COX pumps 2 protons in the P → F step but only 1 in the F → O transition.

Kinetics. There are obvious quantitative differences between the kinetics of electrogenic proton transfer coupled to the P → F and F → O transitions as the former is markedly faster. Deconvolution of the P → F electrogenesis into individual exponents indicates two possible solutions with two or three components for the KCN-sensitive phase, of which the three-exponent approximation is definitely better. Ultimate discrimination between these solutions as well as specific assignment of the individual intraprotein charge (proton) transfer steps resolved in this work must await high-quality time-resolved spectroscopic measurements taken under comparable conditions.

So far, there has been only one work published on the time-resolved heme absorbance changes in bovine COX following single-electron reduction of compound P (*24*). At

the level of two-exponential approximation, our data are in fair agreement. As no attempt was made in ref *24* to deconvolute the absorbance traces associated with heme *a* reoxidation to more than two exponents, comparison of those data with our best-fit solution (three exponents) is not possible.

Differences in the Kinetics of the Electrogenic P → F Transition in the Rapid Reduction and Rapid Oxidation Experiments. Electrogenic proton transfer associated with photoreduction of P to F as measured in this work is much slower than the charge translocation phase with an overall τ of ~0.2 ms assigned to the P → F transition during oxidation of the fully reduced COX by oxygen (*21*). Accordingly, the optically measured P → F transition is significantly slower in the case of RuBpy-induced photoreduction of compound P (*24*) as compared to the P → F step resolved in the oxidation of the fully reduced COX by oxygen (*11*). The discrepancy can be due to different electronic configurations of the P states under those conditions. Compound P generated during oxidation of the fully reduced COX by oxygen and denoted as P_R (subscript R stands for the reduced initial state of COX) is believed to contain reduced Cu_B (*10*, *11*), although, as rightly emphasized by one of the reviewers of this work, direct evidence for the redox state of Cu_B in this intermediate is still missing. In compound P formed by the CO bubbling method or during oxidation by oxygen of the so-called mixed-valence COX (compound P_M, where M stands for the mixed-valence initial state of the enzyme), Cu_B is in all probability oxidized. Therefore, comparison of our data [as well as of the data of Nilsson (*24*) obtained under conditions very similar to those of our work] with the results in refs *10*, *11*, and *21* may indicate that the redox state of Cu_B affects the rate of redox transition of heme a_3 from the P to F state.

The simplest possibility is that the reduced Cu_B serves itself as a fast immediate electron donor to heme a_3-bound oxygen in compound P_R and that electron transfer to the oxygen intermediate from heme *a* is slower in experiments with photoreduction of the P_M state by RuBpy. Another possible explanation is that the redox state of Cu_B controls the connection of the heme a_3-bound oxygen intermediate with the input proton channel (pathway), the reduced state of Cu_B enabling fast proton delivery from the N phase required for the redox transition of P to F (*6*). In particular, there is likely to be a hydroxide anion coordinated to Cu_B in the oxidized enzyme (*52*), and reduction of Cu_B has been calculated to result in protonation of this hydroxide to water (*53*), in agreement with the original proposal of Mitchell (*14*). As suggested in ref *6*, this water could serve as an immediate donor of a proton required to neutralize addition of an electron to the heme a_3−oxene complex in compounds P and F, the availability of this proton controlling the rate of the redox reaction at the heme a_3 site (*54*).

In addition to this mechanistic difference potentially inherent in reactions of P_R and P_M, it should be kept in mind that in contrast to this work, the two charge translocation phases observed by Verkhovsky et al. (*21*) during the oxidation of the fully reduced COX by oxygen and assigned to the P → F and F → O transitions have not been resolved into individual electrogenic reactions. Each of their phases represents superposition of several individual processes with a rather complicated timing (e.g., onset of the 45 μs electrogenic electron transfer from Cu_A to heme *a* follows the ca. 100 μs oxidation of heme *a* by the binuclear center). This circumstance limits interpretation of the data in ref *21* as well as comparison of those data with the results presented here. In particular, if there are any slow partial electrogenic steps with a τ of >1 ms coupled thermodynamically to the P → F transition in the flow flash experiments, like the 1.5 and 7 ms phases observed in this work, these steps would simply merge with the slower F → O part of the process under the experimental conditions of Verkhovsky et al. (*21*).

ACKNOWLEDGMENT

Thanks are due to Dr. T. V. Vygodina and A. Kirichenko for a kind gift of COX. It is our pleasure to thank Dr. D. L. Zaslavskiy and Dr. I. Smirnova for their collaboration at the initial stages of the RuBpy/COX project in this laboratory. We are also indebted to Dr. Zaslavskiy for critical reading of the manuscript of this paper and to Prof. V. P. Skulachev for his interest in this work.

REFERENCES

1. Wikström, M., Krab, K., and Saraste, M. (1981) *Cytochrome Oxidase−A Synthesis*, Academic Press, New York.
2. Babcock, G. T., and Wikström, M. (1992) *Nature 356*, 301−309.
3. Ferguson-Miller, S., and Babcock, G. T. (1996) *Chem. Rev. 96*, 2889−2907.
4. Michel, H., Behr, J., Harrenga, A., and Kannt, A. (1998) *Annu. Rev. Biophys. Biomol. Struct. 27*, 329−356.
5. Konstantinov, A. A., Siletskiy, S. A., Mitchell, D., Kaulen, A. D., and Gennis, R. B. (1997) *Proc. Natl. Acad. Sci. U.S.A. 94*, 9085−9090.
6. Konstantinov, A. (1998) *J. Bioenerg. Biomembr. 30*, 121−130.
7. Wikström, M., and Morgan, J. E. (1992) *J. Biol. Chem. 267*, 10266−10273.
8. Fabian, M., and Palmer, G. (1995) *Biochemistry 34*, 1534−1540.
9. Rich, P., and Moody, A. J. (1997) in *Treatise on Bioelectrochemistry* (Graber, P., and Milazzo, G., Eds.) Vol. 3 (Bioenergetics), pp 419−456, Birkhauser, Basel, Switzerland.
10. Morgan, J. E., Verkhovsky, M. I., and Wikstrom, M. (1996) *Biochemistry 35*, 12235−12240.
11. Sucheta, A., Georgiadis, K. E., and Einarsdóttir, O. (1997) *Biochemistry 36*, 554−565.
12. Kitagawa, T., and Ogura, T. (1997) in *Progress in Inorganic Chemistry* (Karlin, K. D., Ed.) pp 431−479, Wiley, New York.
13. Vygodina, T. V., and Konstantinov, A. A. (1988) *Ann. N.Y. Acad. Sci. 550*, 124−138.
14. Mitchell, P. (1988) *Ann. N.Y. Acad. Sci. 550*, 185−198.
15. Wikström, M. (1989) *Nature 338*, 776−778.
16. Rich, P. R. (1995) *Aust. J. Plant Physiol. 22*, 479−486.
17. Iwata, S., Ostermeier, C., Ludwig, B., and Michel, H. (1995) *Nature 376*, 660−669.
18. Wikstrom, M., Morgan, J. E., and Verkhovsky, M. (1998) *J. Bioenerg. Biomembr. 30*, 139−145.
19. Vygodina, T. V., Capitanio, N., Papa, S., and Konstantinov, A. A. (1997) *FEBS Lett. 412*, 405−409.
20. Zaslavsky, D., Kaulen, A., Smirnova, I. A., Vygodina, T. V., and Konstantinov, A. A. (1993) *FEBS Lett. 336*, 389−393.
21. Verkhovsky, M. I., Morgan, J. E., Verkhovskaya, M., and Wikstrom, M. (1997) *Biochim. Biophys. Acta 1318*, 6−10.
22. Wikström, M., Bogachev, A., Finel, M., Morgan, J. E., Puustinen, A., Raitio, M., Verkhovskaya, M., and Verkhovsky, M. I. (1994) *Biochim. Biophys. Acta 1187*, 106−111.
23. Michel, H. (1998) *Proc. Natl. Acad. Sci U.S.A. 95*, 12819−12824.
24. Nilsson, T. (1992) *Proc. Natl. Acad. Sci. U.S.A. 89*, 6497−6501.

25. Drachev, L. A., Kaulen, A. D., and Skulachev, V. P. (1978) *FEBS Lett. 87*, 161−167.
26. Drachev, L. A., Kaulen, A. D., Semenov, A. Y., Severina, I. I., and Skulachev, V. P. (1979) *Anal. Biochem. 96*, 250−262.
27. Dracheva, S. M., Drachev, L. A., Konstantinov, A. A., Semenov, A. Y., Skulachev, V. P., Arutjunjan, A. M., Shuvalov, V. A., and Zaberezhnaya, S. M. (1988) *Eur. J. Biochem. 171*, 253−264.
28. Zaslavsky, D. L., Smirnova, I. A., Siletsky, S. A., Kaulen, A. D., Millett, F., and Konstantinov, A. A. (1995) *FEBS Lett. 359*, 27−30.
29. Siletsky, S. A., Kaulen, A. D., and Konstantinov, A. A. (1997) *Eur. Biophys. J. 26*, 98.
30. Fowler, L. R., Richardson, S. H., and Hatefi, Y. (1962) *Biochim. Biophys. Acta 64*, 170−173.
31. MacLennan, D. H., and Tzagoloff, A. (1965) *Biochim. Biophys. Acta 96*, 166−168.
32. Hinkle, P. C. (1979) *Methods Enzymol. 55*, 751−776.
33. Tsofina, L. M., Liberman, E. A., Vigodina, T. V., and Konstantinov, A. A. (1985) *Biol. Membr. 2*, 1108−1115.
34. Skulachev, V. P. (1988) *Membrane Bioenergetics*, Springer, Berlin.
35. Provencher, S. W. (1976) *Biophys. J. 16*, 27−50.
36. Vygodina, T., and Konstantinov, A. (1989) *Biochim. Biophys. Acta 973*, 390−398.
37. Weng, L., and Baker, G. M. (1991) *Biochemistry 30*, 5727−5733.
38. Fabian, M., and Palmer, G. (1995) *Biochemistry 34*, 13802−13810.
39. Vygodina, T. V., Schmidmiyer, K., and Konstantinov, A. A. (1992) *Biol. Membr. 9*, 677−692.
40. Zaslavskiy, D. L. (1994) Mechanism of membrane potential generation by cytochrome c oxidase, Ph.D. Thesis, Moscow State University, Moscow, Russia.
41. Nicholls, P., and Chanady, G. A. (1981) *Biochim. Biophys. Acta 634*, 256−265.
42. Junemann, S., Meunier, B., Gennis, R. B., and Rich, P. (1997) *Biochemistry 36*, 14456−14464.
43. Moody, A. J. (1996) *Biochim. Biophys. Acta 1276*, 6−20.
44. Wrigglesworth, J. M., Elsden, J., Chapman, A., Van der Water, N., and Grahn, M. F. (1988) *Biochim. Biophys. Acta 93*, 452−464.
45. Yoshikawa, S., Shinzawa-Itoh, K., Nakashima, R., Yaono, R., Inoue, N., Yao, M., Fei, M. J., Libeu, C. P., Mizushima, T., Yamaguchi, H., Tomizaki, T., and Tsukihara, T. (1998) *Science 280*, 1723−1729.
46. Hinkle, P., and Mitchell, P. (1970) *Bioenergetics 1*, 45−60.
47. Rich, P. R., West, I. C., and Mitchell, P. (1988) *FEBS Lett. 233*, 25−30.
48. Mitchell, R., Mitchell, P., and Rich, P. R. (1992) *Biochim. Biophys. Acta 1101*, 188−191.
49. Zaslavsky, D., Sadoski, R. C., Wang, K., Durham, B., Gennis, R. B., and Millett, F. (1998) *Biochemistry 37*, 14910−14916.
50. Moody, A. J., and Rich, P. R. (1990) *Biochim. Biophys. Acta 1015*, 205−215.
51. Gennis, R. (1998) *Proc. Natl. Acad. Sci. U.S.A. 95*, 12747−12749.
52. Fann, Y. C., Ahmed, I., Blackburn, N. J., Boswell, J. S., Verkhovskaya, M. L., Hoffman, B. M., and Wikström, M. (1995) *Biochemistry 34*, 10245−10255.
53. Kannt, A., Lancaster, C. R. D., and Michel, H. (1998) *Biophys. J. 74*, 708−721.
54. Fenwick, C. W., English, A. M., and Wishart, J. F. (1997) *J. Am. Chem. Soc. 119*, 4758−4764.

BI982614A